



HAL
open science

Ab Initio Screening of Zeolite Y Formulations for Efficient Adsorption of Thiophene in Presence of Benzene

Etienne Paul Hessou, Hicham Jabraoui, Ibrahim Khalil, Marie-Antoinette Dziurla, Michael Badawi

► **To cite this version:**

Etienne Paul Hessou, Hicham Jabraoui, Ibrahim Khalil, Marie-Antoinette Dziurla, Michael Badawi. Ab Initio Screening of Zeolite Y Formulations for Efficient Adsorption of Thiophene in Presence of Benzene. *Applied Surface Science*, 2021, 541, pp.148515. 10.1016/j.apsusc.2020.148515 . hal-03603431

HAL Id: hal-03603431

<https://hal.univ-lorraine.fr/hal-03603431>

Submitted on 3 Feb 2023

HAL is a multi-disciplinary open access archive for the deposit and dissemination of scientific research documents, whether they are published or not. The documents may come from teaching and research institutions in France or abroad, or from public or private research centers.

L'archive ouverte pluridisciplinaire **HAL**, est destinée au dépôt et à la diffusion de documents scientifiques de niveau recherche, publiés ou non, émanant des établissements d'enseignement et de recherche français ou étrangers, des laboratoires publics ou privés.



Distributed under a Creative Commons Attribution - NonCommercial 4.0 International License

16 **ABSTRACT**

17

18 In the context of deep desulfurization of transport fuels, the present work aimed at identifying
19 a suitable material for the selective removal of thiophene from fuels. Dispersion corrected
20 density functional theory (DFT) calculations have been carried out in order to investigate the
21 adsorption of benzene and thiophene in various faujasite zeolite formulations including DAY,
22 HY, LiY, NaY, KY, CsY, Cu(I)Y, Cu(II)Y, Ag(I)Y, Zn(II)Y, and FAU containing Lewis acid
23 sites (LAS) (defect or extra-framework). Bearing-LAS FAU, Cu(I)Y, Cu(II)Y, Zn(II)Y, CsY,
24 and HY showed a higher affinity towards thiophene adsorption. In particular, thiophene is
25 more adsorbed on defect LAS than benzene by 17.7 kJ/mol, suggesting that this zeolite could
26 be chosen as a suitable candidate for the optimal selective adsorption of thiophene in the
27 presence of benzene. In terms of regenerability, all formulations can be safely used (except
28 the one containing extra-framework Lewis acid sites) as they can limit the activation of the C-
29 S bond of thiophene. Considering both adsorption selectivity and sorbent regenerability
30 criteria, faujasites containing defect Lewis acid sites could be chosen as a good compromise
31 to perform a selective adsorption of thiophene in presence of benzene.

32 **Keywords:** Desulfurization, porous, cation, faujasite, DFT, sulfur

33

1. Introduction

The environmental legislation of many countries requires a reduction of the sulfur contents of gasoline and diesel fuels from 400-500 to 0.1-0.2 ppm [1–3], since sulfur-bearing compounds present in commercial fuels contribute to catalyst poisoning during petroleum refining, and to toxic SO_x emissions during fuel combustion in vehicles [4,5]. Thus, deep desulfurization of transport fuels is currently a major world research topic [6–9]. Several efficient technologies already exist such as hydrodesulfurization (HDS) [10,11], extractive desulfurization (EDS) [12], reactive adsorption desulfurization (RADS) [13], oxidative desulfurization (ODS) [14], and adsorptive desulfurization (ADS) [15]. Sulfur compounds are present in fuels as thiols, thioethers and thiophenic species. HDS appears as an efficient technology for thiol and thioether removal, but the process is inefficient for the elimination of thiophenic compounds such as 4,6-dimethyldibenzothiophene which is the most refractory compound to HDS [16]. Moreover, HDS can generate H₂S, which is inhibitory for the deep hydrodesulfurization of the most refractory compounds [17]. Adsorption desulfurization (ADS) can be considered as one of the most promising processes to ultra-clean diesel and gasoline under moderate conditions (ambient temperature and atmospheric pressure) [4,8,15,16,18–21]. Its success is due to the development of highly selective sorbents showing a higher affinity for sulfur compounds than for other major fuel components, and to other criteria such as an excellent adsorption capacity and good sorbent reusability [20–25]. However, the adsorption of sulfur species on sorbents undergoes a strong competition on the adsorption sites with desired aromatics, such as benzene. Commercially available sorbents tested are zeolites, activated charcoal, and activated alumina [26–31]. The zeolite ZSM-5 was shown to be more selective for thiophene than for benzene, toluene, and p-xylene [32]. However, its limited pore size (5.2 to 5.6 Å [33]) sterically hinders or excludes the adsorption of bulky sulfur compounds presenting more than one aromatic ring. Faujasite type zeolites (FAU) which have larger pore sizes and

60 volumes should be more suitable than ZSM-5 for the adsorption of aromatic sulfur
61 compounds. They present a large supercage of 11.0 x 13.0 Å with a large pore opening of 7.4
62 x 7.4 Å, numerous adsorption sites in the supercages, and excellent thermal stability [6,8,34–
63 37].

64 To be selected for ADS technology, sorbents need to combine both high selectivity and good
65 regeneration ability. These two criteria can be estimated by determining the sorbent affinity
66 for various desirable and undesirable molecules present in fuels. Using molecular orbital
67 (MO), Yang et al. [38] investigated π -complexation between thiophene/benzene and transition
68 metals. They also explored the selectivity and reversibility of π -complexation. However, the
69 interactions between thiophene and transition metals are governed by π -complexation, which
70 makes its separation from aromatic hydrocarbons too difficult. Moreover, numerous studies
71 have shown a strong competition between aromatic and thiophenic compounds [17,19,28] for
72 adsorption on various sorbents such as H-ZSM5, H-Beta, HY, AgY, CuY, NaY, H-USY, Na-
73 ZSM-5, activated carbon, and modified activated alumina. Experimental studies have
74 demonstrated that benzene [8] and toluene [39,40] inhibit the adsorption of thiophene in HY
75 zeolites. Using nine types of zeolites, including FAU, FER, and MFI, Zeng et al. [17]
76 investigated the selective adsorption of thiophene in the presence of benzene as a model for
77 aromatic molecules, and showed a strong competition between benzene and thiophene. In
78 fact, in binary mixtures, the sorbent selectivity for thiophene highly depends on pore size,
79 with the optimum pore diameter being between 4.6 and 5.0 Å. In the same context, Duan et al.
80 [18] showed that the efficiency of sulfur compounds removal decreased in the presence of
81 benzene and o-xylene. Using several sorbents including Ag-Y, Cu-Y, Na-Y, H-USY, Na-
82 ZSM-5, activated carbon, and modified activated carbon, Takahashi et al. [28] experimentally
83 investigated benzene/thiophene adsorption. They reported excellent adsorption performances

84 in terms of adsorption and separation capacity for Cu-Y and Ag-Y. However, these results
85 were given without molecular explanations.

86 Density Functional Theory (DFT) calculations have been widely used for identifying suitable
87 zeolite formulations for selective trapping applications such as phenol separation from toluene
88 for the purification of biofuels [34,41–44], trapping of iodine species released during nuclear
89 incidents [45–47], and the separation of NO_x and CO from H₂O and CO₂ for the prevention of
90 harmful emissions from diesel engines in confined spaces [48].

91 The present work aims at providing new insights into the capture of thiophene by FAU type
92 zeolites in the presence of benzene, using dispersion corrected periodic DFT calculations,
93 with taking in account van der Waals (vdW) interactions. More precisely, our objectives are
94 to highlight the influence of the compensating charge cation of the zeolite for thiophene
95 adsorption, and to identify the most efficient FAU formulation, in terms of selectivity and
96 regenerability, for thiophene adsorption in the presence of benzene. Selected formulations are
97 as follows: DAY (Si/Al=∞), D-LAS (Defect Lewis acid site of a Faujasite) [41], EX LAS
98 (Extra-framework Lewis acid site) [41], and the cationic forms HY, LiY, NaY, KY, CsY,
99 Cu(I)Y, Ag(I)Y, Zn(II)Y, Cu(II)Y (Si/Al ratio of 2.43). To our knowledge, there is no DFT
100 investigation dedicated to this issue.

101 The present paper is organized as follows: the first part describes in details our
102 computational procedure; the second part presents and discusses the obtained results, with
103 focusing on the potential inhibitory effect of benzene on thiophene adsorption; finally, the
104 third and last part outlines the main conclusions of the present work.

105

106 **2. Computational details**

107

108 *2.1 Methods*

109

110 Thiophene and benzene adsorption onto FAU zeolites were investigated using the Vienna Ab-
111 initio Simulation Package (VASP) [49]. For these tasks, our DFT calculations employed the
112 PBE functional and projector augmented plane wave (PAW) method [50,51] with a chosen
113 plane wave cutoff energy of 450 eV. Kohn-Sham equations were solved iteratively until the
114 energy difference between cycles became lower than 10^{-6} eV, while the Gaussian smearing
115 was fixed to 0.1 eV. Sampling of the Brillouin zone was limited to the Γ -point. FAU
116 structures were entirely optimized until all the forces fall below 0.01 eV/Å per atom. In order
117 to account for the vdW interactions, the PBE+TS/HI level of theory [52,53] was used. This
118 method has been proven to describe accurately ionic systems such as cationic zeolites
119 [41,48,54]. Adsorption phenomena were evaluated with determining the interaction energy
120 ΔE_{int} between a molecule and a FAU formulation, as indicated in our previous works [54–59].

121

122 *2.2 Structural model*

123 The FAU structure is made up of cuboctahedron sodalite units connected to each other by
124 hexagonal prisms (D6R), leading to the formation of large empty cavities well known as
125 supercages. Interconnections between supercages and their hexagonal windows (6MR) form
126 the porosity of the FAU structures. The pure siliceous structure (DAY) is crystallized within
127 the Fd3m symmetry space group [60] and its supercell structure has the lattice parameters of
128 $a=b=c = 25.028 \text{ \AA}$ (576 atoms, Si₁₉₂O₃₈₄) and $\alpha = \beta = \gamma = 90^\circ$ [61]. By means of the DFT
129 approach, it is difficult in terms of current computational efforts to study the FAU supercell.
130 Therefore, primitive rhombohedral FAU have been used, containing only 144 atoms and
131 represented by two supercages and eight hexagonal windows connecting sodalite cages with
132 supercages, in line with previous studies [62–64]. Twelve FAU structures have been
133 investigated, namely DAY, cation exchange faujasites MY (Si/Al=2.43), where M= H, Li,
134 Na, K, Cs, Cu (I), Ag (I), Zn (II), Cu (II), D-LAS and EX-LAS. DAY is a pure siliceous

135 structure with a Si/Al ratio of ∞ exhibiting a high hydrophobicity [65]. D-LAS is modeled by
136 an excess of negative charge around the placement of the atoms of AlO_4 in FAU (Si/Al = 47;
137 resulting from a simple substitution of Si^{4+} by Al^{3+}) [41,66], while EX-LAS is represented by
138 the substitution of the three Si^{4+} by three Al^{3+} in a 6MR window, and the addition of an extra
139 framework Al^{3+} cation in order to achieve total neutrality in FAU [41].

140

141 **3. Results and discussion**

142 *3.1. Adsorption of benzene and thiophene in FAU zeolites*

143

144 The present part provides a systematic DFT investigation of thiophene and benzene
145 adsorption on the following FAU formulations: DAY, D-LAS and EX-LAS Lewis acid site
146 models, and MY (where M= H, Li, Na, K, Cs, Cu (I), Ag (I), Zn (II), Cu (II)). Calculations
147 were performed using the TS/HI level of theory (PBE+TS/HI). Adsorption configurations are
148 reported in Table S1 (supporting information) and Fig. 1, while total interaction energies are
149 shown in Table 1 and Fig. 2.

150 *3.1.1. Adsorption of thiophene*

151 In DAY, both the sulfur atom and the aromatic ring contribute together to the adsorption of
152 thiophene with ΔE_{int} of 41.5 kJ/mol. This adsorption is controlled by the interactions of the
153 center of a 6MR window of DAY with carbon atoms in thiophene at distances of 3.70-3.94 Å,
154 and with the sulfur atom at a distance of 4.21 Å. For any other FAU formulation, ΔE_{int}
155 thiophene is between 2 and 4 times higher than for DAY.

156 In HY, ΔE_{int} of thiophene is of 90.9 kJ/mol. This adsorption is governed by the interactions of
157 the protonated sites in HY, with the sulfur atom at a distance of 3.29 Å, and with carbons at
158 distances of 2.13 to 3.81 Å (Table S1).

159 For LiY, NaY, KY, and CsY, ΔE_{int} of thiophene are of 64.6 kJ/mol, 76.2 kJ/mol, 81.6 kJ/mol,
160 and 99.2 kJ/mol, respectively. These results indicate a particular behavior where the total

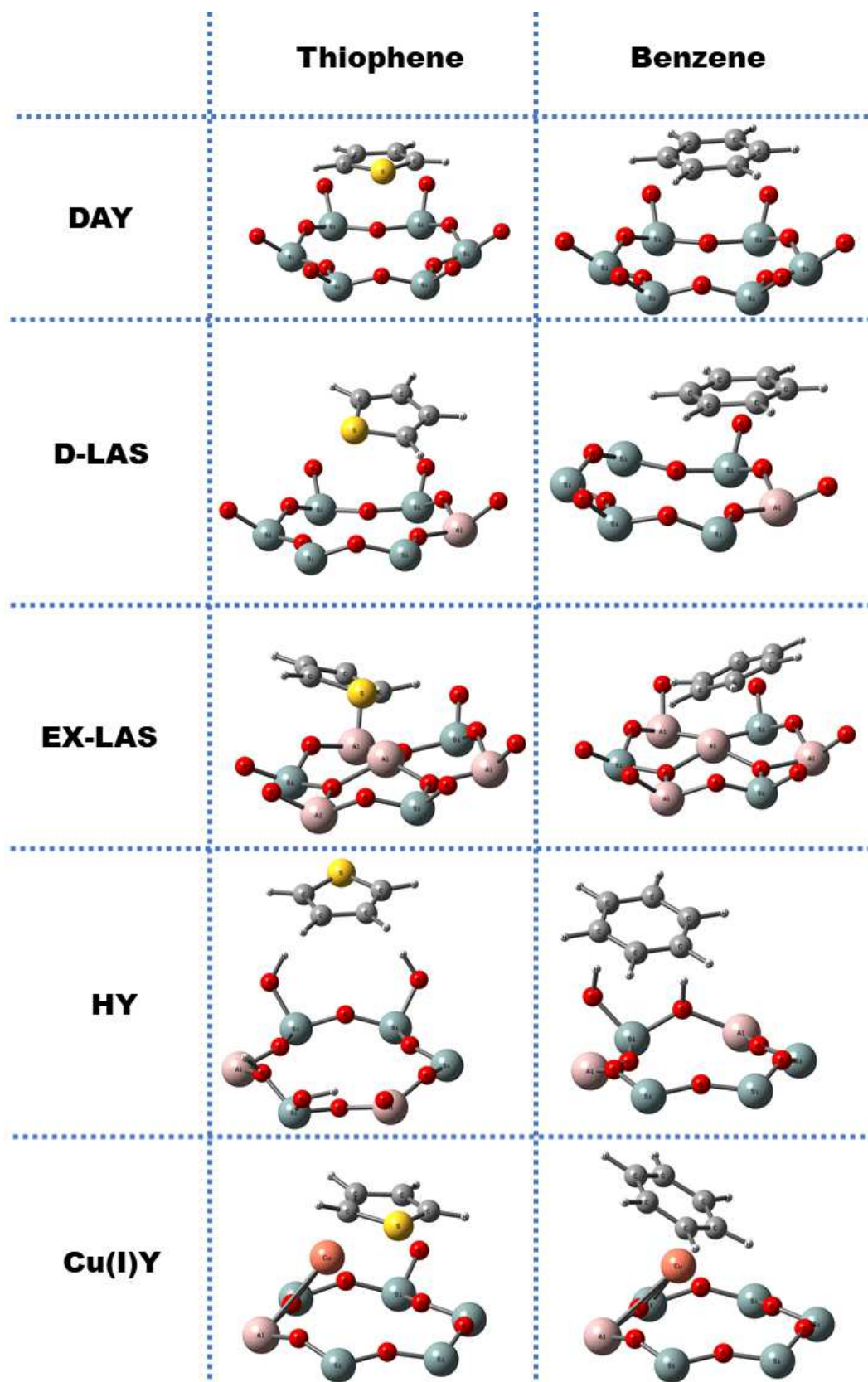
161 interaction energy of thiophene with alkali-FAU increases with the size of the alkali cation.
162 Moreover, our results are in agreement with Takahashi *et al.* [28] who indicated adsorption
163 enthalpies of thiophene in H-USY (high Si/Al) and NaY at room temperature of 46 and 82
164 kJ/mol, respectively. Adsorption configurations show that Li⁺, Na⁺, K⁺ and Cs⁺ interact with
165 thiophene via the sulfur atom at distances of 3.38 Å, 3.15 Å, 3.42 Å and 3.79 Å respectively,
166 and via its carbons at distances of 2.50-3.20 Å, 2.80-3.00 Å, 3.17-3.45 Å, 3.58-3.79 Å,
167 respectively (Table S1). The exchange of alkali cations with transition metal cations (Cu(I),
168 Cu(II), Ag(I), or Zn(II)) results in a significant increase in the affinity of thiophene for FAU
169 zeolites as shown by ΔE_{int} which are of 138.8 kJ/mol for Cu(I), 79.3 kJ/mol for Cu(II)Y,
170 107.3 for Ag(I)Y, and 123.5 kJ/mol for Zn(II)Y. Our results are in agreement with those
171 obtained by Oliveira *et al.* [67] which indicated a strong adsorption of thiophene on transition
172 metals by comparison with the Na⁺ cation. In these sorbents, cationic transition metals Cu(I),
173 Cu(II), Zn(II), and Ag(I) interact with the sulfur atom of thiophene at distances of 3.12 Å,
174 3.71 Å, 3.29 Å, and 3.33 Å respectively, and with its carbons at distances of 2.01-3.40 Å,
175 3.02-3.68 Å, 2.27-3.71 Å, and 2.37-3.58 Å, respectively (Table S1).

176 For D-LAS and EX-LAS formulations, ΔE_{int} of thiophene are of 112.1 kJ/mol and 172.9
177 kJ/mol, respectively. The highest adsorption energy of thiophene is observed with EX-LAS.
178 Considering D-LAS, its 6MR structure interacts with thiophene via the sulfur atom at a
179 distance of 3.76 Å, and also via carbons at distances of 2.86-3.85 Å. EX-LAS interacts with
180 the sulfur atom of thiophene at a distance 3.14 Å and also with its carbons at distances of
181 2.13-3.87 Å. Moreover, interactions between EX-LAS and thiophene are closer than those
182 observed between D-LAS and thiophene, showing that thiophene interacts more closely with
183 EX-LAS than with D-LAS.

184 These results show a strong affinity of thiophene for EX-LAS and Cu(I)Y. Interactions
185 between thiophene and other zeolite formulations decrease in the following order: ZnY > D-

186 LAS \approx Ag(I) > CsY \approx HY. This trend is in good agreement with experimental data reported
187 by Takahashi et al. [28]. Moreover, other experimental data [67] have shown that thiophene is
188 more adsorbed on transition metals than on alkali metals.

189



190

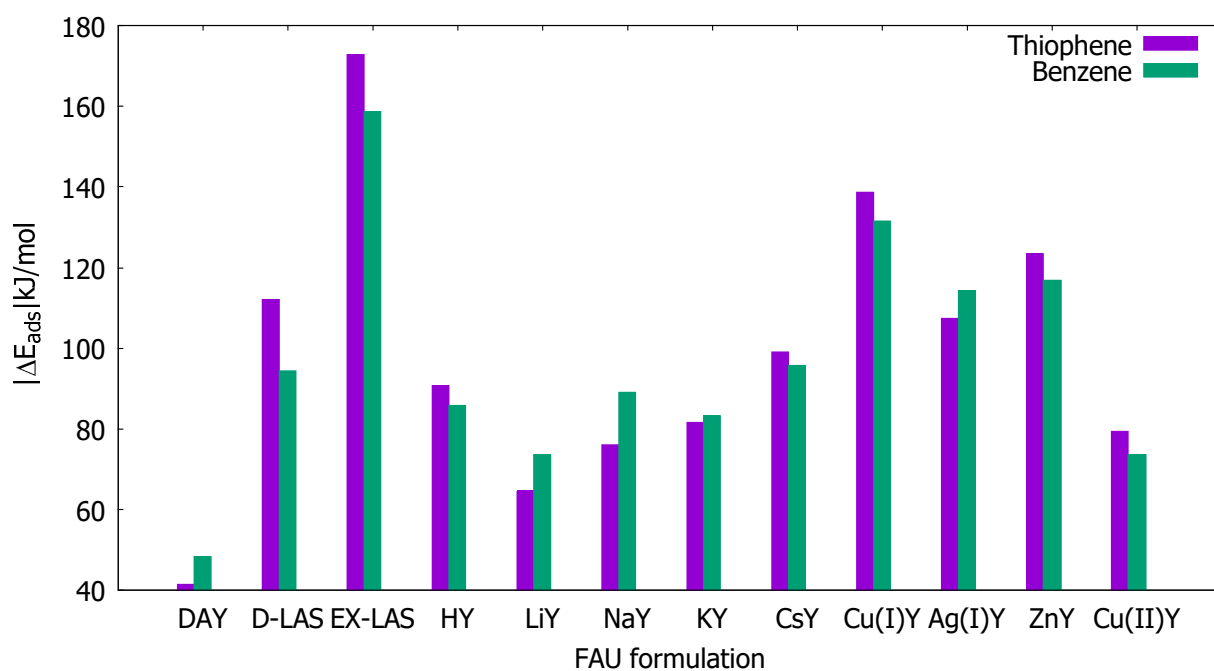
191 **Fig. 1.** Adsorption configurations of thiophene and benzene in DAY, HY, Cu(I)Y, D-LAS,
 192 and EX-LAS. For the sake of clarity, only the 6MR window surrounding the cation and the
 193 molecules is displayed. Blue, red, pink, white, gray and yellow balls represent silicon,
 194 oxygen, aluminum, hydrogen, carbon, and sulfur atoms, respectively.

195

196 **Table 1.** Computed total interaction energies. $|\Delta E_{\text{int}} \text{ (kJ/mol)}|$ of benzene and thiophene in DAY, MY
 197 (Si/Al=2.43) and FAU bearing either D-LAS (Si/Al=47) or EX-LAS (Si/Al=15).
 198

	$ \Delta E_{\text{int}} \text{ (kJ/mol)} $	
	Thiophene	Benzene
DAY	41.5	48.5
D-LAS	112.1	94.4
EX-LAS	172.9	158.6
HY	90.9	85.7
LiY	64.6	73.5
NaY	76.2	89.2
KY	81.6	83.3
CsY	99.2	95.8
Cu(I)Y	138.8	131.4
Ag(I)Y	107.3	114.2
Zn(II)Y	123.5	116.8
Cu(II)Y	79.3	73.6

199



200

201 **Fig. 2.** Total interaction energies of thiophene and benzene molecules, in DAY, D-LAS-
 202 bearing FAU, EX-LAS-bearing FAU, HY, LiY, NaY, KY, CsY, Cu(I)Y, Ag(I)Y, Zn(II)Y,
 203 and Cu(II)Y.

204

205 3.1.2. Adsorption of benzene

206 In DAY, benzene interacts with the center of a 6MR window via its carbon atoms at distances
 207 of 3.58-3.93 Å. The total interaction energy calculated for benzene and DAY (48.5 kJ/mol) is

208 the lowest value observed. Indeed, FAU zeolites with any kind of charge compensating cation
209 or Lewis acid site in their structure exhibit ΔE_{int} with benzene of about 2 to 3 times higher
210 than for DAY. It is already known that the aromatic components can strongly interact over the
211 zeolitic acid sites [68–72], as well as the adsorption strength of these molecules
212 monotonically increases with the cation content [73,74].

213 For HY and NaY, the interaction energies with benzene are 85.7 kJ/mol and 89.2 kJ/mol,
214 respectively. These values are respectively 37.2 and 40.7 kJ/mol higher than for DAY. For
215 LiY, KY and CsY, ΔE_{int} with benzene are 73.5, 83.3, and 95.8 kJ/mol, respectively, which are
216 respectively 25 to 47 kJ/mol higher than for DAY. This trend is consistent with an ONIOM
217 (Own N-layered Integrated molecular Orbital and molecular Mechanics) study on the
218 adsorption of benzene in alkali-exchanged FAU and ZSM-5 zeolites [75]. Moreover,
219 experimental determinations of the adsorption enthalpy of benzene with NaY at room
220 temperature estimated values of about 76 kJ/mol [76,77]. Since a correction of 10 kJ/mol is
221 necessary for extrapolating the adsorption energy at 0 K to an adsorption enthalpy at 300 K
222 [34], our calculations of the total interaction energy at 0K are in good agreement with
223 experimental results. In HY, we found 2 protons interacting with carbons of the aromatic ring
224 of benzene at distances of 2.15-3.50 Å (Table S1). However, Li^+ , Na^+ , K^+ , and Cs^+ interact
225 with carbons of the aromatic ring of benzene at distances of 2.60-2.93 Å, 2.85-2.88 Å, 2.98-
226 3.39 Å, and 3.59-3.67 Å, respectively (Table S1).

227 For Cu(I)Y and Cu(II)Y, ΔE_{int} with benzene are 131.4 kJ/mol and 73.6 kJ/mol, respectively.
228 These values are 82.9 kJ/mol and 25.1 kJ/mol higher than for DAY. In these cases, Cu(I) and
229 Cu(II) cations interact with the carbon atoms of the aromatic ring of benzene respectively at
230 distances of 2.04-3.23 Å, and 2.98-3.43 Å. Moreover, Cu (I) results in a higher total
231 interaction energy than Cu (II), showing that the oxidation state of the copper cation has a
232 clear effect on benzene adsorption in FAU. These results indicate that the interaction of

233 benzene with Cu(I) is more stable than with Cu(II). They are in accordance with Kung studies
234 [78] which reported that at high oxidation states, metals act as weak Lewis acid sites, resulting
235 in a weak interaction energy with adsorbed molecules. In addition, using FTIR spectra
236 Archipov et al. [79] showed that copper undergoes a reduction from Cu(II) to Cu(I) during the
237 adsorption of benzene.

238 For AgY and Zn(II)Y, ΔE_{int} with benzene are 114.2 kJ/mol and 116.8 kJ/mol, respectively. In
239 these sorbents, Ag(I) and Zn(II) interact with carbons of the aromatic ring of benzene at
240 distances of 2.38-3.59 Å and 2.39-3.61 Å, respectively (Table S1). Hence, transition metals
241 Cu, Ag and Zn show a high total interaction energy with benzene, with Cu exhibiting the
242 highest one. Again, our theoretical investigations are in agreement with previous experimental
243 results indicating room temperature adsorption enthalpies of benzene with CuY and AgY of
244 approximately 91.2 kJ/mol and 84.1 kJ/mol, respectively [28].

245 For D-LAS, the total interaction energy with benzene is 94.4 kJ/mol, which is 45.9 kJ/mol
246 higher than for DAY. Finally, the highest ΔE_{int} of benzene is observed with EX-LAS (158.6
247 kJ/mol).

248 Therefore, benzene adsorption with FAU formulations decreased as follows: bearing-EX-LAS
249 FAU > Cu(I)Y > Zn(II)Y \approx Ag(I)Y > bearing-D-LAS FAU \approx CsY > NaY > HY > KY > LiY
250 \approx Cu(II)Y > DAY. Benzene adsorption in different sorbents is performed through interactions
251 between charge compensating cations or 6MR (in DAY) and the aromatic cycle of benzene
252 (Table S1). Our present results are in line with some studies from the literature. Indeed,
253 Takahashi et al. [28] combined experimental determinations and molecular orbital
254 calculations for investigating the adsorption of benzene into several sorbents, including Ag-Y,
255 Cu-Y, Na-Y, and H-USY. Their results showed that benzene highly adsorbs on Cu and Ag
256 cations through π -complexation. Performing an experimental study, Archipov et al. [79]

257 suggested that benzene adsorption on transition metals is favored by Brønsted sites in Y
258 zeolite.

259

260 *3.2. Selectivity of thiophene adsorption on FAU zeolites in the presence of benzene*

261 The previous results (parts 3.1.1. and 3.1.2.) provided individual details on the adsorption of
262 thiophene and benzene in various zeolite formulations. Plotting the interaction energies of
263 benzene and thiophene with the various sorbents (Fig. 2) allows a comparison of the sorbent
264 affinities for these two molecules.

265 In HY, CsY, Cu(II)Y, Cu(I)Y, and Zn(II)Y, thiophene is slightly more adsorbed than benzene
266 by 5.2 kJ/mol, 3.4 kJ/mol, 5.7 kJ/mol, 7.4 kJ/mol, 6.7 kJ/mol, respectively. However, in LiY,
267 NaY, KY, and Ag(I)Y, benzene is slightly more adsorbed than thiophene by 8.9 kJ/mol, 13.0
268 kJ/mol, 1.7 kJ/mol, and 6.9 kJ/mol, respectively. Such energy differences are too low to
269 conclude about the sorbent selectivity towards thiophene or benzene. On the other hand,
270 thiophene is more adsorbed than benzene by 17.7 kJ/mol on D-LAS, suggesting an
271 outstanding trapping performance for D-LAS towards thiophene. Similarly, EX-LAS could be
272 a potential candidate for the selective adsorption of thiophene (energy difference of 14.3
273 kJ/mol). However, its interaction energy with thiophene (172.9 kJ/mol) might be too high to
274 allow a straightforward regeneration of the sorbent.

275 In general, we can clearly suggest that the two zeolite formulations, D-LAS and EX-LAS,
276 present a much higher affinity for thiophene than for benzene. They both display Lewis acid
277 sites. Therefore, we suggest the use of zeolites with a large amount of Lewis acid sites for a
278 selective trapping of thiophene in presence of benzene. Noteworthy, based on the results of
279 our current paper, other theoretical approaches could be performed for a limited selection of
280 formulations to study high coverage such as GCMC and MD simulations, and of course,
281 dedicated experiments could also be performed.

282 3.3. Evaluation of the regenerability of zeolite formulations

283 In addition to the adsorption selectivity criterion, it is also necessary to consider the
284 possibility of chemical reactions between adsorbed thiophene and the investigated
285 formulations as well as the formation of by-products, which would reduce the trapping
286 efficiency and then make the regenerability of the sorbent more difficult [80,81]. To check
287 this point, we analyzed the length of the two S-C bonds (S-C₁ and S-C₄ as labeled in Fig. 3) in
288 thiophene in its gaseous phase (before adsorption), and during adsorption over different
289 formulations. Indeed, three possible situations can arise during adsorption: 1) the first S-C
290 bond remains as in the gas phase (or decrease a little) and the second is lengthened, 2) both S-
291 C bonds in thiophene are lengthened, 3) both S-C bonds keep the same distance during
292 adsorption as in the gas phase. In the first two situations, the elongation of the S-C bond up to
293 dissociation could result in the molecule destruction, and in completely modifying the degree
294 of freedom of sulfur atoms. Ultimately, sulfur atoms of thiophene could be released and
295 precipitate with chemical species present in the adsorption sites. On the other hand, in
296 situation 1, breaking one S-C bond could allow the capture of the sulfur atom in the
297 adsorption site, and facilitate breaking of the second S-C bond. In our investigations, analysis
298 of the bond lengths before and after adsorption showed the following results:

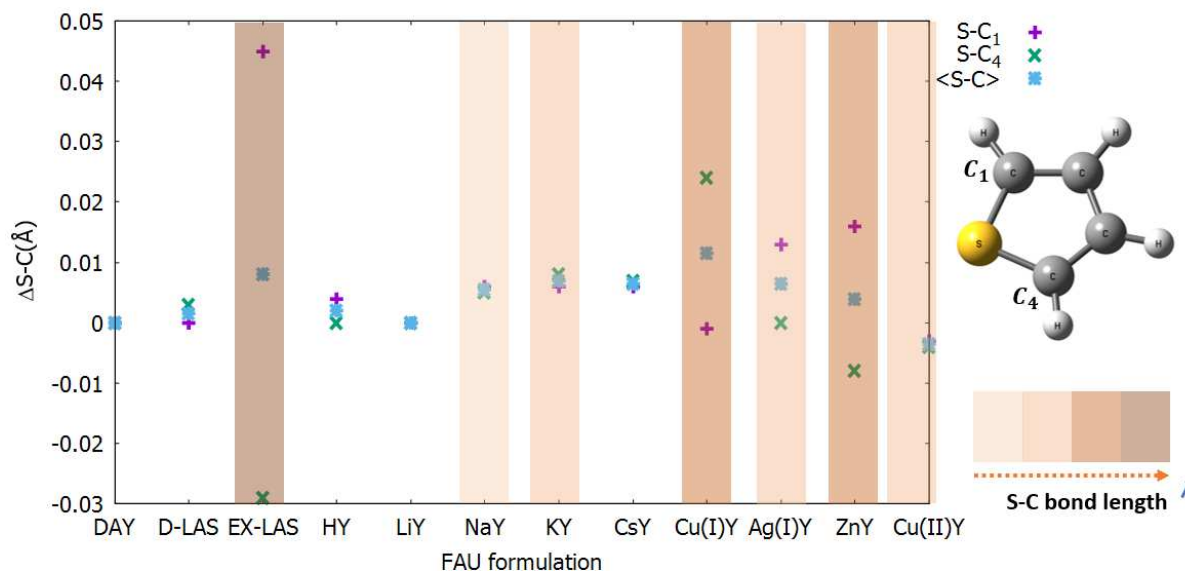
- 299 • In EX-LAS, an elongation of the S-C bond was observed upon adsorption of
300 thiophene with the order of magnitude of 0.045 Å.
- 301 • In Cu(I)Y, Ag(I)Y, and Zn(II)Y, the S-C bond length was larger upon adsorption than
302 in the gas phase, by around 0.025Å, 0.016Å, and 0.018Å, respectively.
- 303 • In HY, LiY, NaY, KY, CsY, Cu(II)Y, DAY, and D-LAS, the S-C bond lengths were
304 roughly similar in the gas phase and upon adsorption.

305 Except for EX-LAS, no significant difference was observed in the S-C bond length, between
306 the gas phase and upon adsorption (no more than 0.03 Å), which ensures that dissociation of

307 thiophene cannot occur after adsorption. This means that in terms of regenerability, all studied
308 formulations could be safely used for the adsorption of thiophene, except EX-LAS.

309

310



311

312 **Fig. 3.** S-C bond length of thiophene in gas phase and upon adsorption.

313

314

315 4. Conclusions

316 In the context of the deep desulfurization of transport fuels, our work aimed at identifying
317 suitable faujasite (FAU) Y formulations for the selective adsorption of thiophene in the
318 presence of benzene. Using periodic, vdW-corrected DFT calculations, we systematically
319 studied the interactions of benzene and thiophene in DAY, FAU containing either Defect
320 Lewis acid sites (D-LAS) or Extra framework Lewis acid sites (EX-LAS), and MY where M
321 = H, Li, Na, K, Cs, Cu(I), Cu(II), Ag(I), and Zn(II).

322 Our main results can be summarized as follows:

- 323 (1) Benzene is adsorbed in any FAU formulation through π -interactions, respectively
324 represented by π -stacking of the aromatic ring on 6MR in DAY, by the interaction of 2

325 protons with the aromatic ring in HY, by M-aromatic ring interactions in MY (M = Li,
326 Na, K, Cs, Cu(I), Cu(II), Ag(I), and Zn(II)), by Al-aromatic ring interactions in EX-
327 LAS, and by π -stacking of the aromatic ring on the 6MR containing the negative charge
328 excess in D-LAS.

329 (2) The affinity of zeolites towards benzene decreases in the following order: bearing-EX-
330 LAS FAU > Cu(I)Y > Zn(II)Y \approx Ag (I)Y > bearing-D-LAS FAU \approx CsY > NaY > HY
331 > KY > LiY \approx Cu(II)Y > DAY.

332 (3) Thiophene also adsorbed through its aromatic ring in the various sorbents. However,
333 the presence of a sulfur atom in its aromatic ring leads to a behavior which is different
334 from benzene.

335 (4) The affinity of thiophene for zeolites decreases in the following order: EX-LAS >
336 Cu(I)Y > Zn(II)Y > D-LAS \approx Ag(I)Y > CsY > HY.

337 Overall, bearing-LAS FAU (D-LAS, and EX-LAS), Cu(I)Y, Cu(II)Y, Zn(II)Y, CsY, and HY
338 present a higher affinity for thiophene than for benzene. In particular, thiophene is more
339 adsorbed on D-LAS than benzene by 17.7 kJ/mol, suggesting an outstanding trapping
340 performance for D-LAS towards thiophene. In terms of regenerability, we have found that all
341 of the formulations can be used safely except EX-LAS. In conclusion, we recommend the
342 incorporation of defect Lewis acid sites in Y formulations to obtain a good compromise
343 between high adsorption selectivity for thiophene in the presence of benzene, and limited C-S
344 bond activation. Alternatively Zn(II)Y and Cu(II)Y could be tested experimentally for the
345 ADS technology.

346

347 **Acknowledgements**

348 This work was granted access to the HPC resources of TGCC under the allocation 2020-
349 A0080910433 made by GENCI. HJ and MB also acknowledge financial support through the

350 COMETE project (COnception in silico de Matériaux pour l'Environnement et l'Energie) co-
351 funded by the European Union under the program "FEDER-FSE Lorraine et Massif des
352 Vosges 2014-2020".

353

354

355 **References**

356

- 357 [1] G.F. Stuntz, F.L. Plantenga, NEW TECHNOLOGIES TO MEET THE LOW SULFUR FUEL CHALLENGE,
358 in: World Petroleum Congress, 2002. <https://www.onepetro.org/conference-paper/WPC-32235>
359 (accessed June 14, 2020).
- 360 [2] K.O. Blumberg, M.P. Walsh, C. Pera, LOW-SULFUR GASOLINE & DIESEL : THE KEY TO LOWER
361 VEHICLE EMISSIONS, in: 2003.
- 362 [3] L. Zavala-Sanchez, I. Khalil, L. Oliviero, J. Paul, F. Maugé, Structure and Quantification of Edge
363 Sites of WS_2/Al_2O_3 Catalysts Coupling IR/CO Spectroscopy and DFT Calculations,
364 ChemCatChem. 12 (2020) 2066–2076. <https://doi.org/10.1002/cctc.201902053>.
- 365 [4] V.M. Bhandari, C. Hyun Ko, J. Geun Park, S.-S. Han, S.-H. Cho, J.-N. Kim, Desulfurization of diesel
366 using ion-exchanged zeolites, Chem. Eng. Sci. 61 (2006) 2599–2608.
367 <https://doi.org/10.1016/j.ces.2005.11.015>.
- 368 [5] I. Bezverkhyy, A. Ryzhikov, G. Gadacz, J.-P. Bellat, Kinetics of thiophene reactive adsorption on
369 Ni/SiO₂ and Ni/ZnO, Catal. Today. 130 (2008) 199–205.
370 <https://doi.org/10.1016/j.cattod.2007.06.038>.
- 371 [6] S. Dang, L. Zhao, Q. Yang, M. Zheng, J. Zhang, J. Gao, C. Xu, Competitive adsorption mechanism
372 of thiophene with benzene in FAU zeolite: The role of displacement, Chem. Eng. J. 328 (2017)
373 172–185. <https://doi.org/10.1016/j.ces.2017.07.011>.
- 374 [7] H. Fu, Y. Wang, T. Zhang, C. Yang, H. Shan, Adsorption and Separation Mechanism of
375 Thiophene/Benzene in MFI Zeolite: A GCMC Study, J. Phys. Chem. C. 121 (2017) 25818–25826.
376 <https://doi.org/10.1021/acs.jpcc.7b07796>.
- 377 [8] Y. Qin, Z. Mo, W. Yu, S. Dong, L. Duan, X. Gao, L. Song, Adsorption behaviors of thiophene,
378 benzene, and cyclohexene on FAU zeolites: Comparison of CeY obtained by liquid-, and solid-
379 state ion exchange, Appl. Surf. Sci. 292 (2014) 5–15.
380 <https://doi.org/10.1016/j.apsusc.2013.11.036>.
- 381 [9] X.-L. Wang, H.-L. Fan, Z. Tian, E.-Y. He, Y. Li, J. Shangguan, Adsorptive removal of sulfur
382 compounds using IRMOF-3 at ambient temperature, Appl. Surf. Sci. 289 (2014) 107–113.
383 <https://doi.org/10.1016/j.apsusc.2013.10.115>.
- 384 [10] R. Prins, V.H.J.D. Beer, G.A. Somorjai, Structure and Function of the Catalyst and the Promoter
385 in Co—Mo Hydrodesulfurization Catalysts, Catal. Rev. 31 (1989) 1–41.
386 <https://doi.org/10.1080/01614948909351347>.
- 387 [11] F. Pelardy, A. Daudin, E. Devers, C. Dupont, P. Raybaud, S. Brunet, Deep HDS of FCC gasoline
388 over alumina supported CoMoS catalyst: Inhibiting effects of carbon monoxide and water, Appl.
389 Catal. B Environ. 183 (2016) 317–327. <https://doi.org/10.1016/j.apcatb.2015.10.026>.
- 390 [12] S. Zhang, Q. Zhang, Z.C. Zhang, Extractive Desulfurization and Denitrogenation of Fuels Using
391 Ionic Liquids, Ind. Eng. Chem. Res. 43 (2004) 614–622. <https://doi.org/10.1021/ie030561+>.
- 392 [13] L. Huang, G. Wang, Z. Qin, M. Dong, M. Du, H. Ge, X. Li, Y. Zhao, J. Zhang, T. Hu, J. Wang, In situ
393 XAS study on the mechanism of reactive adsorption desulfurization of oil product over Ni/ZnO,
394 Appl. Catal. B Environ. 106 (2011) 26–38. <https://doi.org/10.1016/j.apcatb.2011.05.001>.
- 395 [14] H. Mei, B.W. Mei, T.F. Yen, A new method for obtaining ultra-low sulfur diesel fuel via
396 ultrasound assisted oxidative desulfurization☆, Fuel. 82 (2003) 405–414.
397 [https://doi.org/10.1016/S0016-2361\(02\)00318-6](https://doi.org/10.1016/S0016-2361(02)00318-6).
- 398 [15] X. Ma, S. Velu, J.H. Kim, C. Song, Deep desulfurization of gasoline by selective adsorption over
399 solid adsorbents and impact of analytical methods on ppm-level sulfur quantification for fuel
400 cell applications, Appl. Catal. B Environ. 56 (2005) 137–147.
401 <https://doi.org/10.1016/j.apcatb.2004.08.013>.
- 402 [16] R.T. Yang, Adsorbents: Fundamentals and Applications, John Wiley & Sons, 2003.
- 403 [17] Y. Zeng, P.Z. Moghadam, R.Q. Snurr, Pore Size Dependence of Adsorption and Separation of
404 Thiophene/Benzene Mixtures in Zeolites, J. Phys. Chem. C. 119 (2015) 15263–15273.
405 <https://doi.org/10.1021/acs.jpcc.5b03156>.

- 406 [18] L. Duan, X. Gao, X. Meng, H. Zhang, Q. Wang, Y. Qin, X. Zhang, L. Song, Adsorption, Co-
407 adsorption, and Reactions of Sulfur Compounds, Aromatics, Olefins over Ce-Exchanged Y
408 Zeolite, *J. Phys. Chem. C*. 116 (2012) 25748–25756. <https://doi.org/10.1021/jp303040m>.
- 409 [19] A. Chica, K.G. Strohmaier, E. Iglesia, Effects of zeolite structure and aluminum content on
410 thiophene adsorption, desorption, and surface reactions, *Appl. Catal. B Environ.* 60 (2005) 223–
411 232. <https://doi.org/10.1016/j.apcatb.2005.02.031>.
- 412 [20] J. Weitkamp, M. Schwark, S. Ernst, Removal of thiophene impurities from benzene by selective
413 adsorption in zeolite ZSM-5, *J. Chem. Soc. Chem. Commun.* (1991) 1133–1134.
414 <https://doi.org/10.1039/C39910001133>.
- 415 [21] A.J. Hernández-Maldonado, R.T. Yang, Desulfurization of Diesel Fuels by Adsorption via π -
416 Complexation with Vapor-Phase Exchanged Cu(I)-Y Zeolites, *J. Am. Chem. Soc.* 126 (2004) 992–
417 993. <https://doi.org/10.1021/ja039304m>.
- 418 [22] J.H. Kim, X. Ma, A. Zhou, C. Song, Ultra-deep desulfurization and denitrogenation of diesel fuel
419 by selective adsorption over three different adsorbents: A study on adsorptive selectivity and
420 mechanism, *Catal. Today*. 111 (2006) 74–83. <https://doi.org/10.1016/j.cattod.2005.10.017>.
- 421 [23] R.T. Yang, A.J. Hernández-Maldonado, F.H. Yang, Desulfurization of Transportation Fuels with
422 Zeolites Under Ambient Conditions, *Science*. 301 (2003) 79–81.
423 <https://doi.org/10.1126/science.1085088>.
- 424 [24] K. Thomas, I. Khalil, F. Maugé, Selective phenol adsorption from hydrocarbon for ultra-clean
425 biofuel, *Proc. 8 Th Serbian-Croat.-Slov. Symp. Zeolites.* (2019) 41–44.
- 426 [25] L. Alaerts, C.E.A. Kirschhock, M. Maes, M.A. van der Veen, V. Finsy, A. Depla, J.A. Martens, G.V.
427 Baron, P.A. Jacobs, J.F.M. Denayer, D.E. De Vos, Selective Adsorption and Separation of Xylene
428 Isomers and Ethylbenzene with the Microporous Vanadium(IV) Terephthalate MIL-47, *Angew.*
429 *Chem.* 119 (2007) 4371–4375. <https://doi.org/10.1002/ange.200700056>.
- 430 [26] K.X. Lee, G. Tsilomelekis, J.A. Valla, Removal of benzothiophene and dibenzothiophene from
431 hydrocarbon fuels using CuCe mesoporous Y zeolites in the presence of aromatics, *Appl. Catal.*
432 *B Environ.* 234 (2018) 130–142. <https://doi.org/10.1016/j.apcatb.2018.04.022>.
- 433 [27] P. Tan, Y. Jiang, L.-B. Sun, X.-Q. Liu, K. AlBahily, U. Ravon, A. Vinu, Design and fabrication of
434 nanoporous adsorbents for the removal of aromatic sulfur compounds, *J. Mater. Chem. A*. 6
435 (2018) 23978–24012. <https://doi.org/10.1039/C8TA09184F>.
- 436 [28] A. Takahashi, F.H. Yang, R.T. Yang, New Sorbents for Desulfurization by π -Complexation:
437 Thiophene/Benzene Adsorption, *Ind. Eng. Chem. Res.* 41 (2002) 2487–2496.
438 <https://doi.org/10.1021/ie0109657>.
- 439 [29] I. Khalil, C.M. Celis-Cornejo, K. Thomas, P. Bazin, A. Travert, D.J. Pérez-Martínez, V.G. Baldovino-
440 Medrano, J.-F. Paul, F. Maugé, In situ IR-ATR study of the interaction of nitrogen
441 heteroaromatic compounds with HY zeolites: experimental and theoretical approaches,
442 *ChemCatChem*. 12 (2020) 1095–1108. <https://doi.org/10.1002/cctc.201901560>.
- 443 [30] F. Li, L. Song, L. Duan, X. Li, Z. Sun, A frequency response study of thiophene adsorption in
444 zeolite catalysts, *Appl. Surf. Sci.* 253 (2007) 8802–8809.
445 <https://doi.org/10.1016/j.apsusc.2007.05.010>.
- 446 [31] E. Achhal, H. Jabraoui, S. Ouaskit, A. Gibaud, Mesoporous materials from SiO₂ and NiTiO₃, *Mol.*
447 *Cryst. Liq. Cryst.* 634 (2016) 121–129. <https://doi.org/10.1080/15421406.2015.1137271>.
- 448 [32] D.L. King, C. Faz, T. Flynn, Desulfurization of Gasoline Feedstocks for Application in Fuel
449 Reforming, SAE International, Warrendale, PA, 2000. <https://doi.org/10.4271/2000-01-0002>.
- 450 [33] P. Losch, H.R. Joshi, O. Vozniuk, A. Grünert, C. Ochoa-Hernández, H. Jabraoui, M. Badawi, W.
451 Schmidt, Proton Mobility, Intrinsic Acid Strength, and Acid Site Location in Zeolites Revealed by
452 Varying Temperature Infrared Spectroscopy and Density Functional Theory Studies, *J. Am.*
453 *Chem. Soc.* 140 (2018) 17790–17799. <https://doi.org/10.1021/jacs.8b11588>.
- 454 [34] I. Khalil, H. Jabraoui, G. Maurin, S. Lebègue, M. Badawi, K. Thomas, F. Maugé, Selective Capture
455 of Phenol from Biofuel Using Protonated Faujasite Zeolites with Different Si/Al Ratios, *J. Phys.*
456 *Chem. C*. 122 (2018) 26419–26429. <https://doi.org/10.1021/acs.jpcc.8b07875>.

- 457 [35] I. Khalil, K. Thomas, H. Jabraoui, P. Bazin, F. Maugé, Selective elimination of phenol from
458 hydrocarbons by zeolites and silica-based adsorbents—Impact of the textural and acidic
459 properties, *J. Hazard. Mater.* 384 (2020) 121397.
460 <https://doi.org/10.1016/j.jhazmat.2019.121397>.
- 461 [36] Z. Nour, D. Berthomieu, Q. Yang, G. Maurin, A Computational Exploration of the CO Adsorption
462 in Cation-Exchanged Faujasites, *J. Phys. Chem. C*. 116 (2012) 24512–24521.
463 <https://doi.org/10.1021/jp305145s>.
- 464 [37] I. Déroche, G. Maurin, B.J. Borah, S. Yashonath, H. Jobic, Diffusion of Pure CH₄ and Its Binary
465 Mixture with CO₂ in Faujasite NaY: A Combination of Neutron Scattering Experiments and
466 Molecular Dynamics Simulations, *J. Phys. Chem. C*. 114 (2010) 5027–5034.
467 <https://doi.org/10.1021/jp910863z>.
- 468 [38] R.T. Yang, A. Takahashi, F.H. Yang, New Sorbents for Desulfurization of Liquid Fuels by π -
469 Complexation, *Ind. Eng. Chem. Res.* 40 (2001) 6236–6239. <https://doi.org/10.1021/ie010729w>.
- 470 [39] X. Han, H. Li, H. Huang, L. Zhao, L. Cao, Y. Wang, J. Gao, C. Xu, Effect of olefin and aromatics on
471 thiophene adsorption desulfurization over modified NiY zeolites by metal Pd, *RSC Adv.* 6 (2016)
472 75006–75013. <https://doi.org/10.1039/C6RA15914A>.
- 473 [40] H. Li, X. Han, H. Huang, Y. Wang, L. Zhao, L. Cao, B. Shen, J. Gao, C. Xu, Competitive adsorption
474 desulfurization performance over K – Doped NiY zeolite, *J. Colloid Interface Sci.* 483 (2016) 102–
475 108. <https://doi.org/10.1016/j.jcis.2016.08.024>.
- 476 [41] H. Jabraoui, I. Khalil, S. Lebègue, M. Badawi, Ab initio screening of cation-exchanged zeolites for
477 biofuel purification, *Mol. Syst. Des. Eng.* 4 (2019) 882–892.
478 <https://doi.org/10.1039/C9ME00015A>.
- 479 [42] I. Khalil, H. Jabraoui, S. Lebègue, W.J. Kim, L.-J. Aguilera, K. Thomas, F. Maugé, M. Badawi,
480 Biofuel purification: Coupling experimental and theoretical investigations for efficient
481 separation of phenol from aromatics by zeolites, *Chem. Eng. J.* 402 (2020) 126264.
482 <https://doi.org/10.1016/j.cej.2020.126264>.
- 483 [43] S. Gueddida, S. Lebègue, M. Badawi, Assessing the potential of amorphous silica surfaces for
484 the removal of phenol from biofuel: a density functional theory investigation, *J. Phys. Chem. C*.
485 (2020). <https://doi.org/10.1021/acs.jpcc.0c06581>.
- 486 [44] H. Jabraoui, Étude théorique de l'adsorption sélective du phénol par des matériaux zéolithiques
487 pour la purification des biocarburants, phdthesis, Université de Lorraine, 2019. [https://hal.univ-](https://hal.univ-lorraine.fr/tel-02328052)
488 [lorraine.fr/tel-02328052](https://hal.univ-lorraine.fr/tel-02328052) (accessed October 26, 2020).
- 489 [45] S. Chibani, M. Chebbi, S. Lebègue, L. Cantrel, M. Badawi, Impact of the Si/Al ratio on the
490 selective capture of iodine compounds in silver-mordenite: a periodic DFT study, *Phys. Chem.*
491 *Chem. Phys.* 18 (2016) 25574–25581. <https://doi.org/10.1039/C6CP05015H>.
- 492 [46] H. Jabraoui, E.P. Hessou, S. Chibani, L. Cantrel, S. Lebègue, M. Badawi, Adsorption of volatile
493 organic and iodine compounds over silver-exchanged mordenites: A comparative periodic DFT
494 study for several silver loadings, *Appl. Surf. Sci.* 485 (2019) 56–63.
495 <https://doi.org/10.1016/j.apsusc.2019.03.282>.
- 496 [47] E. Hessou, H. Jabraoui, M. Chebbi, S. Chibani, L. Cantrel, M. Badawi, Evaluation of the Inhibiting
497 Effect of Organic Compounds on the Adsorption of Iodine Compounds in Cation-Exchanged
498 Zeolites: A DFT Study, in: A. Kallel, M. Ksibi, H. Ben Dhia, N. Khélifi (Eds.), *Recent Adv. Environ.*
499 *Sci. Euro-Mediterr. Surround. Reg.*, Springer International Publishing, Cham, 2018: pp. 107–109.
500 https://doi.org/10.1007/978-3-319-70548-4_37.
- 501 [48] E.P. Hessou, W.G. Kanhounon, D. Rocca, H. Monnier, C. Vallières, S. Lebègue, M. Badawi,
502 Adsorption of NO, NO₂, CO, H₂O and CO₂ over isolated monovalent cations in faujasite zeolite:
503 a periodic DFT investigation, *Theor. Chem. Acc.* 137 (2018) 161.
504 <https://doi.org/10.1007/s00214-018-2373-2>.
- 505 [49] G. Sun, J. Kürti, P. Rajczyk, M. Kertesz, J. Hafner, G. Kresse, Performance of the Vienna ab initio
506 simulation package (VASP) in chemical applications, *J. Mol. Struct. THEOCHEM.* 624 (2003) 37–
507 45. [https://doi.org/10.1016/S0166-1280\(02\)00733-9](https://doi.org/10.1016/S0166-1280(02)00733-9).

- 508 [50] G. Kresse, D. Joubert, From ultrasoft pseudopotentials to the projector augmented-wave
509 method, *Phys. Rev. B.* 59 (1999) 1758–1775. <https://doi.org/10.1103/PhysRevB.59.1758>.
- 510 [51] P.E. Blöchl, Projector augmented-wave method, *Phys. Rev. B.* 50 (1994) 17953–17979.
511 <https://doi.org/10.1103/PhysRevB.50.17953>.
- 512 [52] T. Bučko, S. Lebègue, J. Hafner, J.G. Ángyán, Improved Density Dependent Correction for the
513 Description of London Dispersion Forces, *J. Chem. Theory Comput.* 9 (2013) 4293–4299.
514 <https://doi.org/10.1021/ct400694h>.
- 515 [53] T. Bučko, S. Lebègue, J.G. Ángyán, J. Hafner, Extending the applicability of the Tkatchenko-
516 Scheffler dispersion correction via iterative Hirshfeld partitioning, *J. Chem. Phys.* 141 (2014)
517 034114. <https://doi.org/10.1063/1.4890003>.
- 518 [54] S. Chibani, M. Chebbi, S. Lebègue, T. Bučko, M. Badawi, A DFT investigation of the adsorption of
519 iodine compounds and water in H-, Na-, Ag-, and Cu- mordenite, *J. Chem. Phys.* 144 (2016)
520 244705. <https://doi.org/10.1063/1.4954659>.
- 521 [55] E.P. Hessou, H. Jabraoui, M.T.A.K. Hounguè, J.-B. Mensah, M. Pastore, M. Badawi, A first
522 principle evaluation of the adsorption mechanism and stability of volatile organic compounds
523 into NaY zeolite, *Z. Für Krist. - Cryst. Mater.* 234 (2019) 469–482. <https://doi.org/10.1515/zkri-2019-0003>.
- 524
- 525 [56] A. Geneyton, Y. Foucaud, L.O. Filippov, N.-E. Menad, A. Renard, M. Badawi, Synergistic
526 adsorption of lanthanum ions and fatty acids for efficient rare-earth phosphate recovery:
527 Surface analysis and ab initio molecular dynamics studies, *Appl. Surf. Sci.* 526 (2020) 146725.
528 <https://doi.org/10.1016/j.apsusc.2020.146725>.
- 529 [57] S. Gueddida, S. Lebègue, M. Badawi, Interaction between transition metals (Co, Ni, and Cu)
530 systems and amorphous silica surfaces: A DFT investigation, *Appl. Surf. Sci.* 533 (2020) 147422.
531 <https://doi.org/10.1016/j.apsusc.2020.147422>.
- 532 [58] A.B. Schvval, A. Juan, G.F. Cabeza, Theoretical study of the role of the interface of Ag₄
533 nanoclusters deposited on TiO₂(110) and TiO₂(101), *Appl. Surf. Sci.* 490 (2019) 343–351.
534 <https://doi.org/10.1016/j.apsusc.2019.05.291>.
- 535 [59] V. Orazi, A. Juan, E.A. González, J.M. Marchetti, P.V. Jasen, DFT study of ethanol adsorption on
536 CaO(0 0 1) surface, *Appl. Surf. Sci.* 500 (2020) 144254.
537 <https://doi.org/10.1016/j.apsusc.2019.144254>.
- 538 [60] W.H. Baur, On the cation and water positions in faujasite, *Am. Mineral.* 49 (1964) 697–704.
- 539 [61] F. Porcher, M. Souhassou, Y. Dusausoy, C. Lecomte, The crystal structure of a low-silica
540 dehydrated NaX zeolite, *Eur. J. Mineral.* (1999) 333–344.
541 <https://doi.org/10.1127/ejm/11/2/0333>.
- 542 [62] E.P. Hessou, M. Ponce-Vargas, J.-B. Mensah, F. Tielens, J.C. Santos, M. Badawi, Dibenzyl
543 Disulfide Adsorption on Cationic Exchanged Faujasites: A DFT Study, *Nanomaterials.* 9 (2019)
544 715. <https://doi.org/10.3390/nano9050715>.
- 545 [63] J.M. Salazar, M. Badawi, B. Radola, M. Macaud, J.M. Simon, Quantum Effects on the Diffusivity
546 of Hydrogen Isotopes in Zeolites, *J. Phys. Chem. C.* 123 (2019) 23455–23463.
547 <https://doi.org/10.1021/acs.jpcc.9b05090>.
- 548 [64] S. Komaty, A. Daouli, M. Badawi, C. Anfray, M. Zaarour, S. Valable, S. Mintova, Incorporation of
549 trivalent cations in NaX zeolite nanocrystals for the adsorption of O₂ in the presence of CO₂,
550 *Phys. Chem. Chem. Phys.* 22 (2020) 9934–9942. <https://doi.org/10.1039/D0CP00111B>.
- 551 [65] B. de Fonseca, J. Rossignol, I. Bezverkhyy, J.P. Bellat, D. Stuerger, P. Pribetich, Detection of VOCs
552 by microwave transduction using dealuminated faujasite DAY zeolites as gas sensitive
553 materials, *Sens. Actuators B Chem.* 213 (2015) 558–565.
554 <https://doi.org/10.1016/j.snb.2015.02.006>.
- 555 [66] L. Benco, T. Bucko, J. Hafner, H. Toulhoat, Ab Initio Simulation of Lewis Sites in Mordenite and
556 Comparative Study of the Strength of Active Sites via CO Adsorption, *J. Phys. Chem. B.* 108
557 (2004) 13656–13666. <https://doi.org/10.1021/jp048056t>.

- 558 [67] M.L.M. Oliveira, A.A.L. Miranda, C.M.B.M. Barbosa, C.L. Cavalcante, D.C.S. Azevedo, E.
559 Rodriguez-Castellon, Adsorption of thiophene and toluene on NaY zeolites exchanged with
560 Ag(I), Ni(II) and Zn(II), *Fuel*. 88 (2009) 1885–1892. <https://doi.org/10.1016/j.fuel.2009.04.011>.
- 561 [68] S. Vanderbeken, E. Dejaegere, K. Tehrani, J. Paul, P. Jacobs, G. Baron, J. Denayer, Alkylation of
562 deactivated aromatic compounds on zeolites. Adsorption, deactivation and selectivity effects in
563 the alkylation of bromobenzene and toluene with bifunctional alkylating agents, *J. Catal.* 235
564 (2005) 128–138. <https://doi.org/10.1016/j.jcat.2005.06.029>.
- 565 [69] I. Daems, P. Leflaive, A. Méthivier, G.V. Baron, J.F.M. Denayer, Influence of Si:Al-ratio of
566 faujasites on the adsorption of alkanes, alkenes and aromatics, *Microporous Mesoporous*
567 *Mater.* 96 (2006) 149–156. <https://doi.org/10.1016/j.micromeso.2006.06.029>.
- 568 [70] S. Chempath, R.Q. Snurr, J.F.M. Denayer, G.V. Baron, Molecular siting in the liquid-phase
569 adsorption of alkane and aromatic mixtures in MFI zeolites: An experimental and molecular
570 modeling study, *Stud. Surf. Sci. Catal.* 154 (2004) 1983–1990. [https://doi.org/10.1016/S0167-](https://doi.org/10.1016/S0167-2991(04)80737-7)
571 [2991\(04\)80737-7](https://doi.org/10.1016/S0167-2991(04)80737-7).
- 572 [71] J.-P. Bellat, J.C. Moise, V. Cottier, C. Paulin, A. Methivier, Effect of Water Content on the
573 Selective Coadsorption of Gaseous *p*-Xylene and *m*-Xylene on the BaY Zeolite, *Sep. Sci. Technol.*
574 33 (1998) 2335–2348. <https://doi.org/10.1080/01496399808545278>.
- 575 [72] V. Cottier, J.-P. Bellat, M.-H. Simonot-Grange, A. Méthivier, Adsorption of *p*-Xylene/*m*-Xylene
576 Gas Mixtures on BaY and NaY Zeolites. Coadsorption Equilibria and Selectivities, *J. Phys. Chem.*
577 *B.* 101 (1997) 4798–4802. <https://doi.org/10.1021/jp9640033>.
- 578 [73] O.M. Dzhigit, A.V. Kiselev, T.A. Rachmanova, Henry's constants, isotherms and heats of
579 adsorption of some hydrocarbons in zeolites of faujasite type with different content of sodium
580 cations, *Zeolites*. 4 (1984) 389–397. [https://doi.org/10.1016/0144-2449\(84\)90017-4](https://doi.org/10.1016/0144-2449(84)90017-4).
- 581 [74] M.A. El-Dib, A.S. Moursy, M.I. Badawy, Role of adsorbents in the removal of soluble aromatic
582 hydrocarbons from drinking waters, *Water Res.* 12 (1978) 1131–1137.
583 [https://doi.org/10.1016/0043-1354\(78\)90061-1](https://doi.org/10.1016/0043-1354(78)90061-1).
- 584 [75] K. Bobuatong, J. Limtrakul, Effects of the zeolite framework on the adsorption of ethylene and
585 benzene on alkali-exchanged zeolites: an ONIOM study, *Appl. Catal. Gen.* 253 (2003) 49–64.
586 [https://doi.org/10.1016/S0926-860X\(03\)00465-4](https://doi.org/10.1016/S0926-860X(03)00465-4).
- 587 [76] D. Barthomeuf, B.-H. Ha, Adsorption of benzene and cyclohexane on faujasite-type zeolites.
588 Part 1.—Thermodynamic properties at low coverage, *J. Chem. Soc. Faraday Trans. 1 Phys.*
589 *Chem. Condens. Phases.* 69 (1973) 2147–2157. <https://doi.org/10.1039/F19736902147>.
- 590 [77] V. Finsy, S. Calero, E. García-Pérez, P.J. Merkling, G. Vedts, D.E. De Vos, G.V. Baron, J.F.M.
591 Denayer, Low-coverage adsorption properties of the metal–organic framework MIL-47 studied
592 by pulse chromatography and Monte Carlo simulations, *Phys. Chem. Chem. Phys.* 11 (2009)
593 3515. <https://doi.org/10.1039/b822247a>.
- 594 [78] M.C. Kung, H.H. Kung, IR Studies of NH₃, Pyridine, CO, and NO Adsorbed on Transition Metal
595 Oxides, *Catal. Rev.* 27 (1985) 425–460. <https://doi.org/10.1080/01614948508064741>.
- 596 [79] T. Archipov, S. Santra, A.B. Ene, H. Stoll, G. Rauhut, E. Roduner, Adsorption of Benzene to
597 Copper in CuHY Zeolite, *J. Phys. Chem. C.* 113 (2009) 4107–4116.
598 <https://doi.org/10.1021/jp805976a>.
- 599 [80] A. Illanes, L. Wilson, G. Tomasello, Effect of modulation of enzyme inactivation on temperature
600 optimization for reactor operation with chitin-immobilized lactase, *J. Mol. Catal. B Enzym.* 11
601 (2001) 531–540. [https://doi.org/10.1016/S1381-1177\(00\)00023-0](https://doi.org/10.1016/S1381-1177(00)00023-0).
- 602 [81] C.Y. Li, L.V.C. Rees, Ion exchange, thermal stability and water desorption studies of faujasites
603 with different Si/Al ratios, *React. Polym. Ion Exch. Sorbents.* 7 (1988) 89–99.
604 [https://doi.org/10.1016/0167-6989\(88\)90129-8](https://doi.org/10.1016/0167-6989(88)90129-8).
- 605

GRAPHICAL ABSTRACT

